The Institute of Space and Astronautical Science
Report SP No.14, December 2000

Gravitationally Lensed Galaxy Number Counts in the Infrared II: Concrete Examples

By

Atsunori YONEHARA*, Kohji YOSHIKAWA*, and Tsutomu T. TAKEUCHI†

(November 1, 2000)

Abstract: Following the concept presented by Takeuchi, Yoshikawa, & Yonehara (2000), we show some concrete examples of number count of lensed galaxies in the infrared. Adopting a simple lens model of cluster of galaxies, we are able to estimate the expected number counts of galaxies. The result tells us that the expected number counts of galaxies around a single cluster are not so large, but in principle, we can discriminate global history of galaxy evolution efficiently at longer waveband, i.e. FIR and/or sub-mm.

1. A MODEL OF CLUSTERS OF GALAXIES AS A GRAVITATIONAL LENS

In this section, we present a model of clusters of galaxies as a gravitational lens and its properties. Throughout this paper, we use the following cosmological parameters:

$$\Omega = 0.3, \quad \Lambda = 0.0, \quad \text{and } H_0 = 75 \text{ km s}^{-1} \text{ Mpc}^{-1}. \tag{1}$$

In general, the mass distribution of clusters of galaxies is hard to be determined and is not simple. The mass distribution is different from cluster to cluster. Fortunately, in the case of a cluster of galaxies with strong gravitational lensing features (e.g. giant luminous arcs), we can determine the mass distribution fairly well. In the final stage of our study, we will have to use such a well determined mass distribution and perform some estimation like the expected number of galaxies. However, for simplicity, we use an ideal lens model for a cluster of galaxies to calculate the expected galaxy number counts as the first step.

1.1 SSIS Model for a Cluster of Galaxies

There are several lens models for clusters of galaxies (e.g. see Hattori, Kneib, & Makino 1999). In the present study, we use one of those models, called "Softened Singular Isothermal Sphere (SSIS)". The SSIS model has an axisymmetric mass distribution, and so, the gravitational lens

* Department of Astronomy, Kyoto University, Sakyo-ku, Kyoto, 606–8502, JAPAN; yonehara@kusastro.kyoto-u.ac.jp
† Division of Particle and Astrophysical Sciences, Nagoya University, Nagoya, 464–8602, JAPAN

effect depends only on the apparent angular separation (θ) from the center of the cluster. The mass enclosed within the radius θ, $M(<\theta)$, of the model is written as follows;

$$M(<\theta) = 2\pi^2 D_{\rm ol}^3 \rho_0 \left(\frac{r_{\rm core}}{D_{\rm ol}}\right) \left(\left(\theta^2 + \left(\frac{r_{\rm core}}{D_{\rm ol}}\right)^2 \right)^{1/2} - \frac{r_{\rm core}}{D_{\rm ol}} \right). \tag{2}$$

Here, $D_{\rm ol}$ is the angular diameter distance between the observer and the lens (i.e. cluster), ρ_0 is the core density of the cluster, and $r_{\rm core}$ is the core radius of the cluster. Thus, the lens equation (relation between the image position (lensed image position; $\vec{\theta}$), and the source position (the image position in the case of lensing; $\vec{\beta}$)) in the above mass distribution can be written as

$$\vec{\beta} = \vec{\theta} - \frac{4GM(<|\vec{\theta}|)}{c^2} \cdot \frac{D_{\rm ls}}{D_{\rm ol} D_{\rm os}} \cdot \frac{\vec{\theta}}{|\vec{\theta}|^2}, \tag{3}$$

where $D_{\rm os}$ and $D_{\rm ls}$ are angular diameter distances between the observer and the source, and between the lens and the source. By using the lens equation, we can easily obtain magnification (A) due to the gravitational lensing effect at any given image position ($\vec{\theta}$) via *Jacobian* matrix, $A(\vec{\theta}) = \det|\frac{\partial \vec{\beta}}{\partial \vec{\theta}}|^{-1}$.

For our estimations, we adopt the following typical parameters for the cluster, $\rho_0 = 1.5 \times 10^{16} M_\odot$ Mpc^{-3} and $r_{\rm core} = 0.08$ Mpc. Furthermore, in order to determine the properties of the gravitational lens, we should also specify the redshift of the lens (i.e. cluster), $z_{\rm ol}$. As many clusters of galaxies with strong gravitational lensing features are already known (see Table 1), we perform our calculation for three values of the lens redshift, $z_{\rm ol} = 0.2$, 0.3, and 0.4.

Table 1: Clusters of galaxies with strong gravitational lensing features and their redshift. See also Hattori, Kneib, & Makino (1999)

redshift	$z_{\rm ol} \sim 0.2$	$z_{\rm ol} \sim 0.3$	$z_{\rm ol} \sim 0.4$
	A2218 ($z_{\rm ol} \sim 0.18$)	AC114 ($z_{\rm ol} \sim 0.31$)	A370 ($z_{\rm ol} \sim 0.37$)
clusters	MS0440+02 ($z_{\rm ol} \sim 0.19$)	MS2137-23 ($z_{\rm ol} \sim 0.31$)	CL0024+1654 ($z_{\rm ol} \sim 0.39$)
	A2390 ($z_{\rm ol} \sim 0.23$)	AC118 ($z_{\rm ol} \sim 0.33$)	

1.2 Properties of the Lens Model

Adopting the above lens model, we can obtain the magnification for any source redshift and position for a given lens redshift.

Contours of the magnification around a cluster for the three cases are shown in Figure 1. There are two distinctive features in contours of large magnification, two horizontal ($\theta =$ *const.* $\simeq 1$) regions and one vertical ($z_{\rm os} =$ *const.*) region. This is a very useful property of the lens because differences are among the three models for galaxy evolution considered by Takeuchi, Yoshikawa, & Yonehara (2000) mainly around the redshift range ~ 1. Therefore, by using the gravitational lens effect of a cluster, differences amongst the three models for galaxy evolution are significantly enhanced and we can, in principle, discriminate the global history of evolution of galaxies.

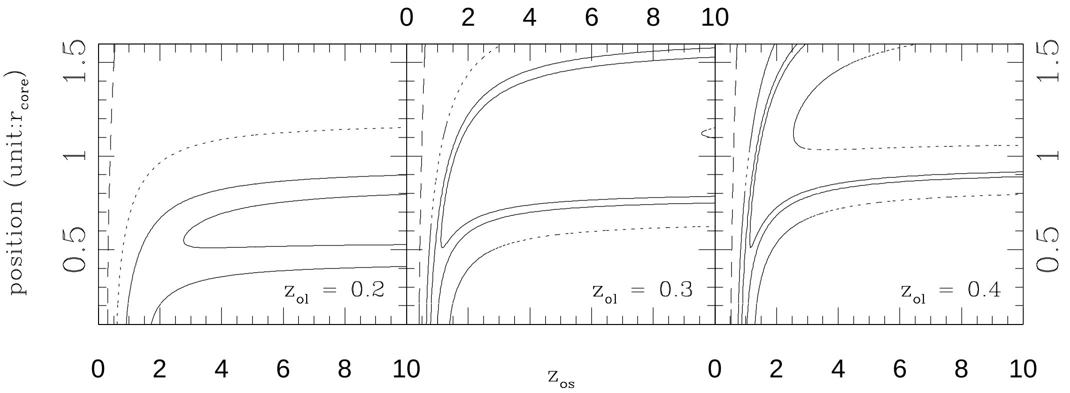

Fig. 1: Contour plots of magnification around a cluster are shown in this figure. Abscissa is the source redshift ($z_{\rm os}$) and the ordinate is the separation from the center of cluster (θ) in unit of the core radius ($r_{\rm core}$). Different lines represent different magnifications (solid: $\times300$, dotted: $\times30$, dashed: $\times3$).

1.3 Comments on Gravitational Lens Effect

Additionally, we note some advantages of the galaxy number counts in the IR wavebands arising from the gravitational lensing by a cluster. Generally, there are two competing effects in the gravitationally-lensed, galaxy number counts; one is flux magnification and the other is image plane stretching, i.e., so-called "*Broadhurst effect*" (e.g. Broadhurst, Taylor, & Peacock 1995). The former effect increases the expected counts of galaxies, because the effective limiting flux density for observation becomes lower and intrinsically faint galaxies turn out to be detectable. On the other hands, the latter effect decreases the expected galaxy number counts; since the observed region of the sky is also magnified, intrinsically smaller region is observed, and the expected galaxy number counts in any given region of the sky become less. According for both effects, the count of galaxies in the optical band is reduced (this effect called "*depletion*") since the Broadhurst effect dominates over the simple flux magnification. Owing to differences in the intrinsic (unlensed) properties of galaxies in the IR and the optical bands, simple flux magnification overcompensates the Broadhurst effect in the IR band. Thus, leading to an increase in the number count of lensed galaxies, at least for the apparently brighter sources, a positive magnification bias will occur in the IR wavebands. Furthermore, simple flux magnification enables us to detect faint galaxies below the detection limit of flux density for the unlensed cases.

2. RESULTS OF OUR ESTIMATION

2.1 Calculations

To get an estimate of the expected galaxy number counts brighter than detection limit S, $N(>S)$, we convolve the magnification factor and intrinsic galaxy number counts;

$$N(>S) = \int_{z_{\rm ol}}^{\infty} dz \frac{dV^2}{d\Omega dz} \int_{\theta_{\rm in}}^{\theta_{\rm out}} 2\pi\theta d\theta \int_{L(S/A(z,\theta),z)}^{\infty} \frac{\phi(z,L')}{A(z,\theta)} dL'. \quad (4)$$

Here, S is observed flux, $\theta_{\rm in}$ and $\theta_{\rm out}$ is inner and outer radius of annulus of the observed region on the sky, L is the luminosity, $\phi(z,L')$ is the comoving number density of galaxies per unit interval in redshift, z, and luminosity, L', V is the volume, and Ω is the solid angle (see also Broadhurst, Taylor, & Peacock 1995).

We integrate the above equation numerically, except for the integration related to θ. For θ integration, we only sum up the area weighted values with separation of $0.1 r_{\rm core}$.

2.2 Expected Galaxy Number Counts

We have calculated the expected galaxy number counts through gravitational lensing by cluster in three wavebands, 50(μm), 100(μm), and 175(μm). Adopted evolution models for galaxies are "model 1", "model 2", and "model 3" described in Takeuchi, Yoshikawa, & Yonehara (2000). The results are shown in figures 2, 3, and 4.

As we have already noted, we can easily see that the expected number counts are increased by an order of magnitude because of the lensing effect at least in the brighter flux density region, say > 0.01Jy. Thus, our number count sensitivity is increased. Moreover, difference between different galaxy evolution models are also enhanced at high flux density region and these difference become reasonable in contrast to the situation for unlensed galaxies. These figures tell us our proposed technique will work. However, in a single cluster, the difference is not so significant, and we should observe around many clusters and perform some statistical analysis to get a clear conclusion. Such work will be undertaken in our future works.

ACKNOWLEDGMENT

This work was partly supported by Research Fellowship of the Japan Society for the Promotion of Science for Young Scientists (9852, AY and 4672, KY).

REFERENCES

Hattori M., Kneib J.P., & Makino F. 1999, in: Prog. Theor. Phys. Suppl. 133, Gravitational Lensing and The High Redshift Universe, ed. K. Tomita & T. Futamase (Kyoto: Prog. Thoer. Phys.), 1

Takeuchi T.T., Yoshikawa K., & Yonehara, A. 2000, this volume

Broadhurst T.J., Taylor A.N., & Peacock J.A. 1995, ApJ, 438, 49

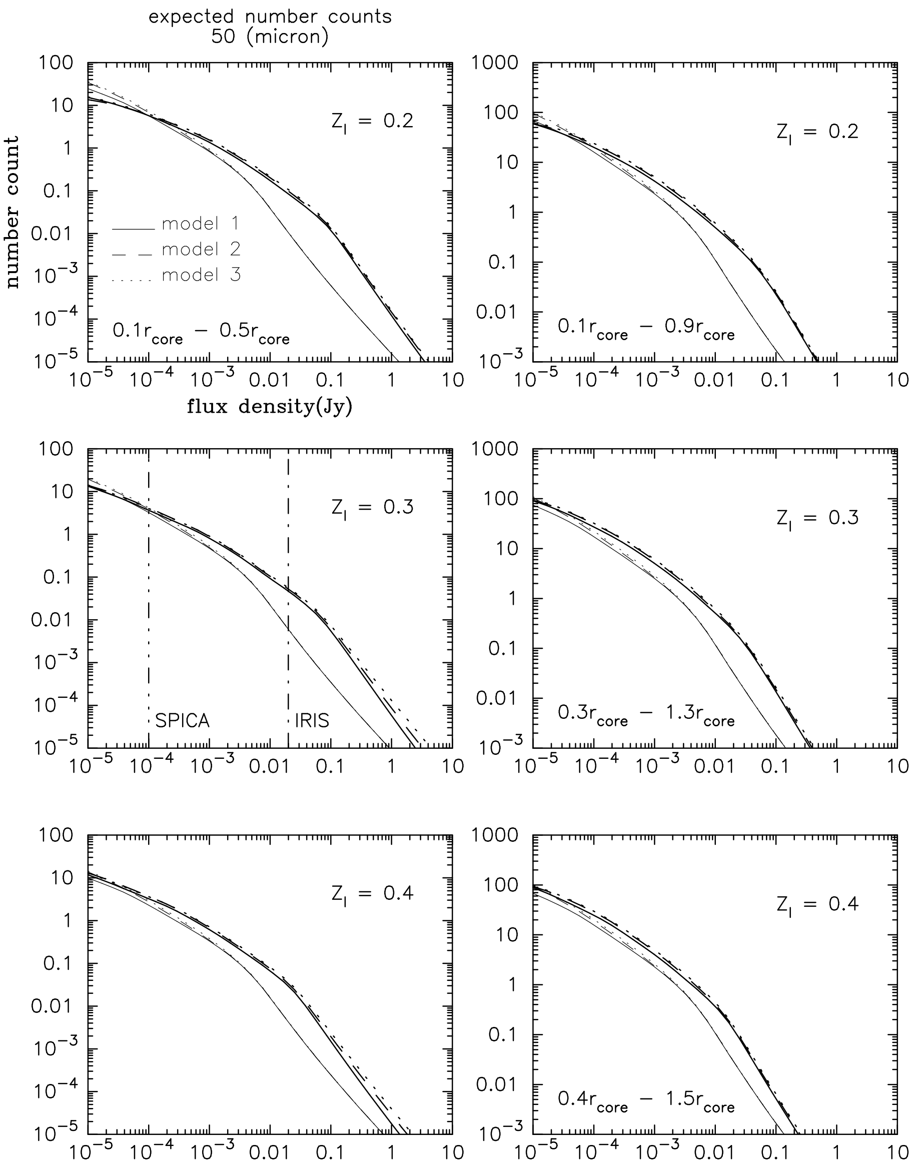

Fig. 2: Expected galaxy number counts through gravitational lens (cluster). In this figure $\lambda = 50\mu m$. Thin and thick solid lines show the expected number counts without lensing, and with lensing. Different line species mean different evolution model (bold is "model 1", dashed is "model 2", and dotted is "model 3"). Upper, middle, and lower panels correspond to the case that the cluster redshift is 0.2, 0.3, and 0.4. Left panels show expected galaxy number counts in annulus region between $0.1r_{\rm core}$ and $0.5r_{\rm core}$ around lensing cluster. Right panels show expected galaxy number counts at different region from left panels (actual regions are specified at left lower part in each panel). Detection limits for some future IR-satellites are also shown by dot-dashed (ASTRO-F), and three dot-dashed (HII/L2) line in the middle left panel.

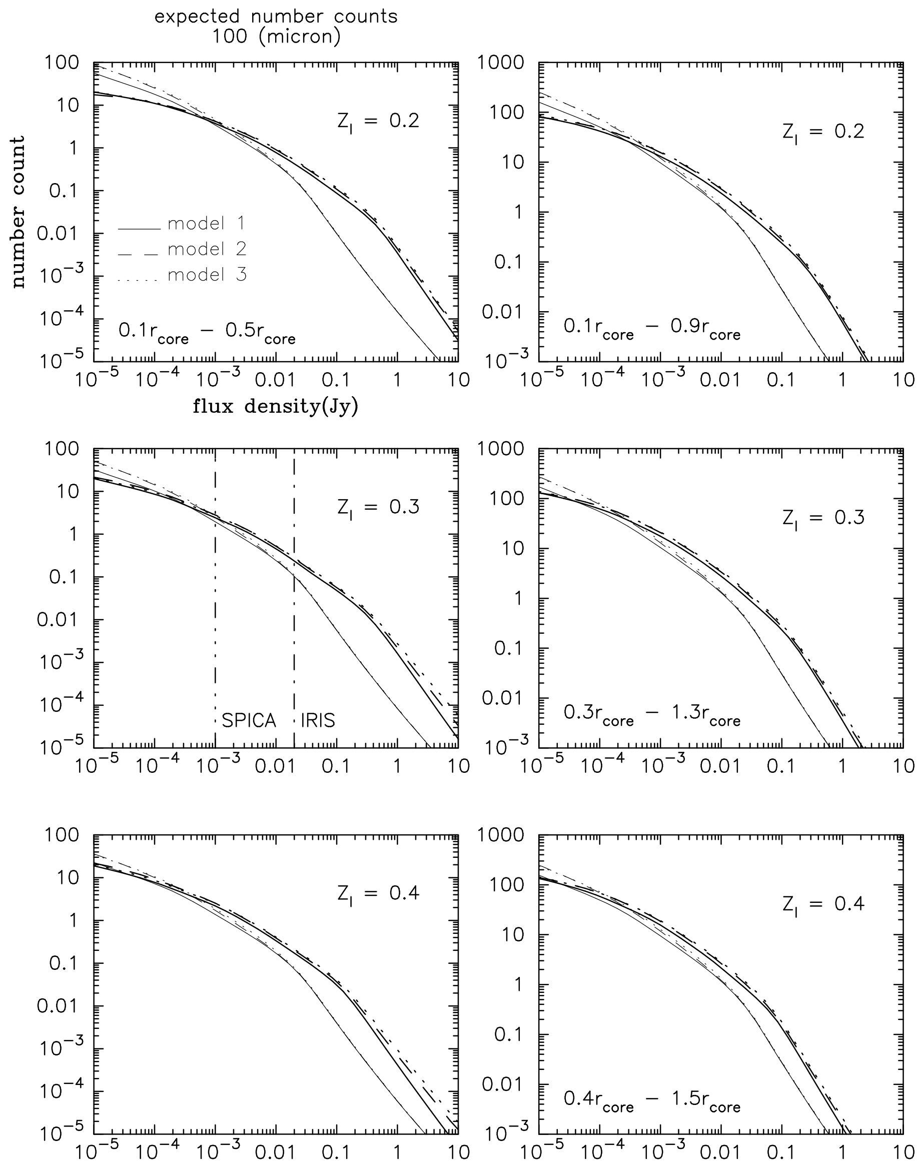

Fig. 3: Same as figure 2, but $\lambda = 100\mu m$.

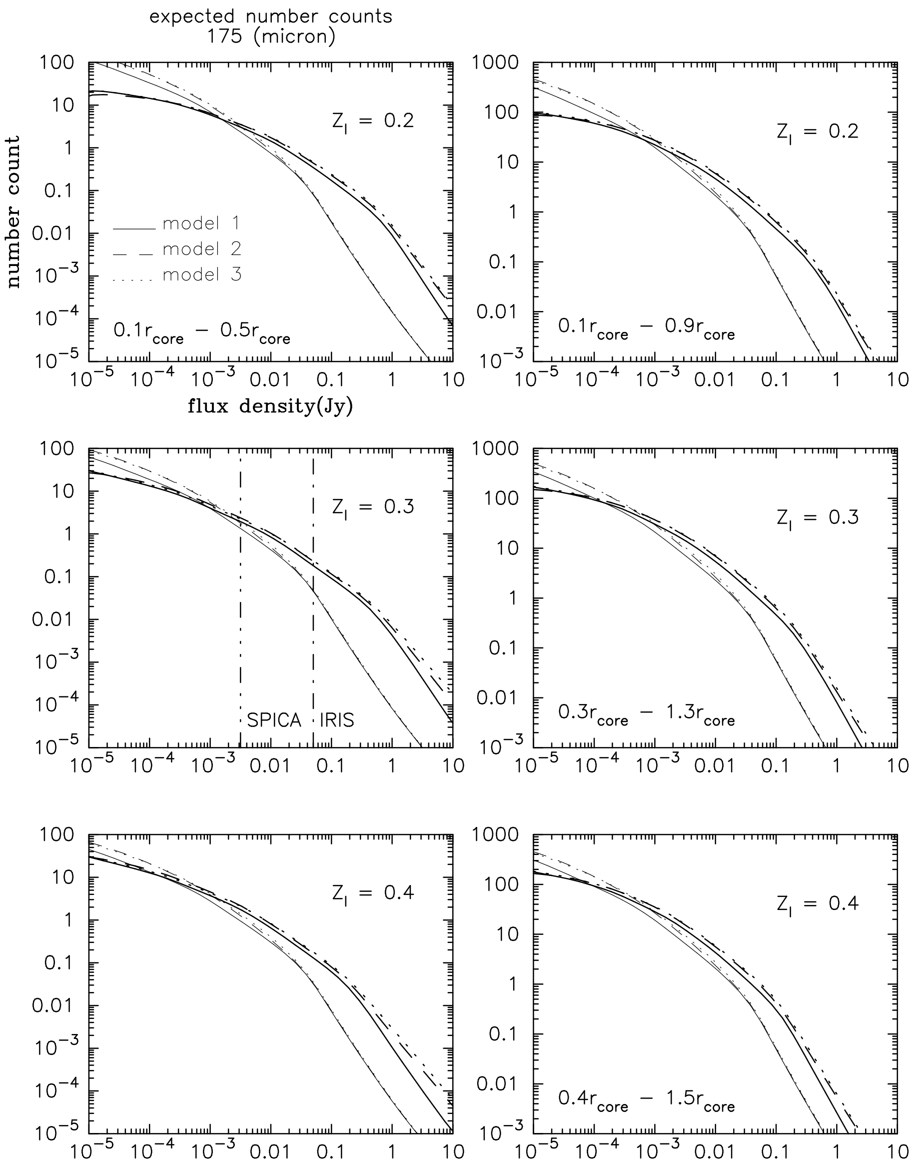

Fig. 4: Same as figure 2, but $\lambda = 175\mu m$.